

Designing the “Search Pathway” in the Development of a New Class of Highly Efficient Stereoselective Hydrosilylation Catalysts

Vincent César,^[a] Stéphane Bellemin-Lapponnaz,^{*[a]} Hubert Wadepohl,^[b] and Lutz H. Gade^{*[a, b]}

Dedicated to Professor Brian F. G. Johnson

Abstract: The direct coupling of oxazolines and N-heterocyclic carbenes leads to chelating C,N ancillary ligands for asymmetric catalysis that combine both an “anchor” unit and a stereodirecting element. Reacting various N-substituted imidazoles with 2-bromo-4(*S*)-*tert*-butyl- and 2-bromo-4(*S*)-isopropoxyloxazoline gave the imidazolium precursors of the stereodirecting ancillary ligands. A library of ten different ligand precursors was obtained by using this simple procedure (65–97% yield). These protoligands were metalated in a subsequent step by reaction with $[\{\text{Rh}(\mu\text{-OtBu})(\text{nbd})\}_2]$ (nbd = norbornadiene), generated in situ from KOtBu and $[\{\text{RhCl}(\text{nbd})\}_2]$ giving the corresponding N-heterocyclic carbene complexes $[\text{RhBr}(\text{nbd})(\text{oxazolonyl-carbene})]$ **4a–j** in good yields. X-ray diffraction studies of two of the rhodium complexes, **4d** and **4j**, established a distorted square-pyramidal coordination geometry with the bromo ligand occupying the apical position. The rhodium–carbene bond length was found to be 2.070(4) Å (**4d**) and 2.012(3) Å (**4j**). Complexes **4a–j**

were treated with AgBF₄ in dichloromethane, giving the active cationic square-planar catalysts for the hydrosilylation of ketones. As a reference reaction for the catalyst optimisation, the hydrosilylation of acetophenone with diphenylsilane was studied and the system optimised with respect to the counterion (BF₄[−]), solvent (THF) and the silane reducing agent (diphenylsilane). The reaction product (1-phenylethanol) was obtained with the highest enantiomeric excess (*ee*) by carrying out the reaction at −60°C, whilst the enantioselectivity drops upon going both to lower and higher temperatures. The observation that the temperature dependence of the *ee* values goes through a maximum indicated a change in the rate-determining step as the temperature is varied. The determination of the initial reaction rate in the hydrosilylation of acetophenone upon vary-

ing the catalyst (**4d**) and substrate concentrations at −55°C established a rate law for the initial conversion which is first-order in both substrates as well as the catalyst ($V_i = k[\mathbf{4}][\text{PhCOMe}][\text{Ph}_2\text{SiH}_2]$). The catalytic system derived from complex **4d** was found to afford high yields and good enantioselectivities in the reduction of various aryl alkyl ketones (acetophenone: 92% isolated yield and 90% *ee*, 2-naphtyl methyl ketone: 99% yield, 91% *ee*). The selectivity for the reduction of prochiral dialkyl ketones is comparable or even superior to the best previously reported for prochiral nonaromatic ketones; whereas cyclopropyl methyl ketone is hydrosilylated with an enantioselectivity of 81% *ee*, the increase of the steric demand of one of the alkyl groups leads to improved *ee*'s, reaching 95% *ee* in the case of *tert*-butyl methyl ketone. Linear chain *n*-alkyl methyl ketones, which are particularly challenging substrates, are reduced in good asymmetric induction, such as 2-octanone (79% *ee*) and even 2-butanone (65% *ee*).

Keywords: carbene ligands • hydrosilylation • N ligands • oxazolines • rhodium

[a] Dr. V. César, Dr. S. Bellemin-Lapponnaz, Prof. L. H. Gade

Laboratoire de Chimie Organométallique
et de Catalyse (UMR 7513)
Institut Le Bel, Université Louis Pasteur
4 rue Blaise Pascal, 67070 Strasbourg (France)
Fax: (+33) 390-241-531
E-mail: bellemin@chimie.u-strasbg.fr
gade@chimie.u-strasbg.fr

[b] Prof. H. Wadepohl, Prof. L. H. Gade

Anorganisch-Chemisches Institut, Universität Heidelberg
Im Neuenheimer Feld 270, 69120 Heidelberg (Germany)
Fax: (+49) 6221-545-609
E-mail: lutz.gade@uni-hd.de

Introduction

The development of catalysts for new chemical transformations or catalytic systems with improved performance for known reactions is one of the key challenges of current chemical research. In practical terms, the quest for successful strategies to solve a given problem occupies centre stage. In a recent perceptive article on the limits of rationality in catalyst development, Hoveyda et al. have pointed out that efficient routes to novel catalysts may be based on the design of a *search pathway* rather than the preconception of an individual catalyst structure derived from a complete mechanistic analysis of a catalytic process.^[1] Such search strategies are conveniently based on highly modular catalyst systems, their basic structural motifs being derived from the available mechanistic insight into the catalytic process combined with the known ligand properties of its components.

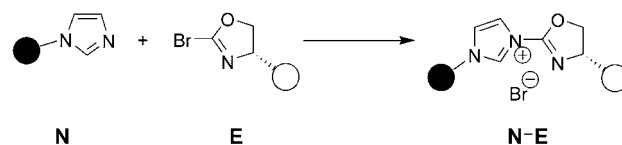
In an optimised “search algorithm”, the ancillary (stereodirecting) ligands are assembled in a single step from readily accessible building blocks. The ligand assembly is followed by a metallation step giving the (pre)catalyst. The coordination of the ancillary ligand to the metal should be kinetically inert in order to give a relatively well-defined active system. Its structure should therefore combine both an “anchor” unit and—in the case of asymmetric catalysis—a stereodirecting element.

N-heterocyclic carbenes^[2] are excellent “anchor” units for late transition metals, which form strong metal–carbon bonds and have thus been widely used in homogeneous catalysis.^[2–4] They are straightforward to synthesise, often chemically more stable than the extensively employed phosphines and may be readily combined with other ligating units, in particular, by the appropriate functionalisation of the N-atoms in their heterocyclic structures.^[4] We recently reported the direct coupling of oxazolines and N-heterocyclic carbenes,^[5] which are modelled on previously studied heterodonor–phosphine stereodirecting ligands for d⁸-M^I/d⁶-M^{III} catalysis.^[6] Their highly modular assembly and metallation is designed according to the search pathway delineated above and was thought to provide an efficient strategy to develop novel chiral catalysts.^[7] In this paper we provide a full account of the “search pathway” leading to a new, highly efficient class of N-heterocyclic carbene-based catalysts for the asymmetric hydrosilylation of prochiral ketones.^[8,9] We also present the potential pitfalls associated with the nonlinearity in the behaviour of an enantioselective catalyst in response to the variation of key reaction parameters. These observations are due to the complexity of the reaction mechanism.

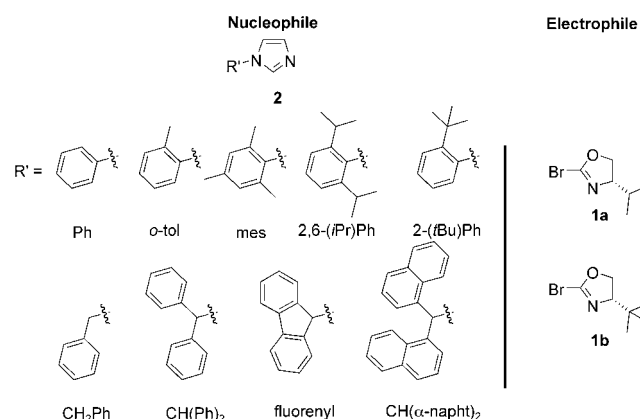
Results and Discussion

Library design: As mentioned above, the ideal strategy for the modular design of a new catalyst is based on essentially a single assembly step of its structural and functional subunits. To this end we directly coupled various N-substituted

imidazoles (**N**), which display nucleophilic reactivity, with 2-bromooxazolines (**E**) to give the imidazolium precursors (**N–E**) of the stereodirecting ancillary ligands. These were metalated in a subsequent step by reaction with alkoxyrhodium complexes as first described by Herrmann et al.^[4a]



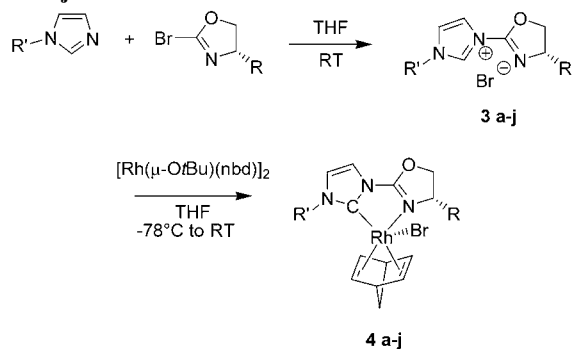
Preparation of the components for the ligand-coupling step and assembly of the stereodirecting ancillary ligands: As indicated, 2-bromooxazolines serve as the electrophiles in the preparation of the imidazolium salts from the respective imidazole precursors. Following the procedure reported by Meyers and Novacek, the reaction of the lithiated oxazoline (*t*BuLi, THF, -78°C) with 1,2-dibromotetrafluoroethane gave the corresponding 2-bromo-4(*S*)-isopropyl oxazoline (**1a**) and 2-bromo-4(*S*)-*tert*-butyl oxazoline (**1b**).^[10,11] Both reagents were isolated by direct bulb-to-bulb distillation from the reaction mixtures giving solutions in THF (usually 75–90 % w/w).



The imidazoles used for this study are depicted above, all of which were prepared by the established synthetic procedures.^[12–14] The imidazolium salts, which served as “protio” ligand precursors, were prepared by direct coupling of the 2-bromooxazolines and the imidazoles in THF at room temperature. The imidazolium salts precipitated as white powders, which are indefinitely stable under an atmosphere of nitrogen and were analytically and spectroscopically pure. A library of ten different ligand precursors was obtained by using this simple procedure (65–97 % yield; Table 1).

Preparation and structure of the rhodium complexes: The reaction of **3a–i** with $[\{\text{Rh}(\mu\text{-O}t\text{Bu})(\text{nbd})\}_2]$ (nbd = norbornadiene), generated in situ from KO t Bu and $[\{\text{RhCl}(\text{nbd})\}_2]$,

Table 1. Synthesis of the imidazolium salts **3a–j** and the rhodium complexes **4a–j**.



3,4	R'	R	3,4	R'	R
a	Ph	<i>t</i> Bu	f	2- <i>t</i> BuC ₆ H ₄	<i>t</i> Bu
b	<i>o</i> -tol	<i>t</i> Bu	g	CH ₂ Ph	<i>t</i> Bu
c	mes	<i>i</i> Pr	h	CHPh ₂	<i>t</i> Bu
d	mes	<i>t</i> Bu	i	fluorenyl	<i>t</i> Bu
e	2,6-(<i>i</i> Pr) ₂ Ph	<i>t</i> Bu	j	CH(napht) ₂	<i>t</i> Bu

yielded the corresponding N-heterocyclic carbene complexes **4a–j** in good yields (above 80%), except for **4i** in which the concurrent deprotonation of the acidic proton of the fluorenyl group lead to partial decomposition (Table 1).^[15] All complexes were purified by recrystallisation from dichloromethane/pentane, characterised by elemental analysis and NMR spectroscopy, and were found to be stable in air. Particularly diagnostic for the formation of the carbene complexes was the observation of the ¹³C NMR resonances of the carbene carbon nuclei,^[4,5] at $\delta = 184\text{--}191$ ppm with coupling constants $J(\text{Rh},\text{C})$ of approximately 55 Hz. Furthermore, a significant oxazoline $\nu(\text{C}=\text{N})$ vibrational band shift to lower wave numbers (of about 20 cm⁻¹) indicated the coordination of the oxazolinyl unit to the metal centre.

Two of rhodium complexes, compounds **4d** and **4j**, were characterised by X-ray diffraction, and their molecular structures are depicted in Figure 1 along with the principal bond lengths and angles. Both complexes possess distorted square-pyramidal coordination geometries with the bromo ligand occupying the apical position. Given this coordination geometry and the arrangement of the ligands, the observation of two diastereomers was in principle possible. However, both in solution and in the solid state, only one diastereoisomer was observed. In the molecular structures of **4d** and **4j** the bromo ligand was found to adopt the same orientation relative to the *tert*-butyl substituent of the ancillary ligand, probably due to steric repulsion between the latter and the norbornadiene ligand. As observed for related compounds, the mesityl ring in compound **4d** is oriented almost orthogonally to the imidazolyl ring (dihedral angle: C10-N3-C11-C12 81.6°).^[15] The rhodium–carbene bond length was found to be 2.070(4) Å and the *trans* influence of the N-heterocyclic carbene is manifested in the difference of Rh–C bond lengths to the C=C units in the norbornadiene (see selected bond data in legend of Figure 1).

Basically the same structural features were observed for compound **4j** (rhodium–carbene bond length: 2.012(3) Å).

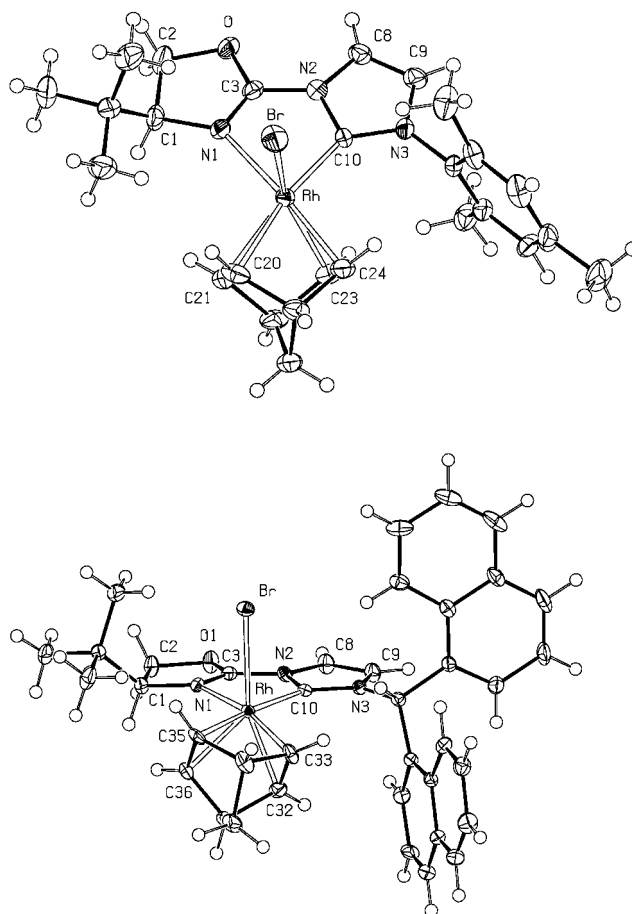


Figure 1. Top: Molecular structure of complex **4d**. Selected bond lengths (Å) and angles (°): Rh–Br, 2.6775(5); Rh–N1, 2.285(3); Rh–C10 2.001(4); Rh–C20/C21, 2.231(4)/2.231(4); Rh–C23/C24, 2.084(4), 2.070(4); N1–Rh–Br, 91.72(9); N1–Rh–C10, 77.0(1); N1–Rh–C20, 113.6(2); N1–Rh–C21, 95.4(2); N1–Rh–C23, 128.3(2); N1–Rh–C24, 168.3(2); C10–Rh–Br, 96.5(1); C20/C24–Rh–Br, 84.8(1)/99.9(1); C21/C23–Rh–Br, 116.4(1)/139.9(1); C20–Rh–C24, 66.4(2); C21–Rh–C23, 65.1(2). Bottom: Molecular structure of complex **4j**. Selected bond lengths (Å) and angles (°): Rh–Br, 2.6914(4); Rh–N1, 2.265(3); Rh–C10, 2.012(3); Rh–C32/C33, 2.097(3)/2.069(3); Rh–C35/C36, 2.218(3)/2.217(3); C32–C33, 1.435(5); C35–C36, 1.384(5); N1–Rh–Br, 89.97(7); N1–Rh–C10, 77.4(1); N1–Rh–C32, 126.2(1); N1–Rh–C33, 166.2(1); N1–Rh–C35, 112.1(1); N1–Rh–C36, 92.5(1); C10–Rh–Br, 90.76(8); C32/C36–Rh–Br, 143.8(1)/119.99(9); C33/C35–Rh–Br, 103.6(1)/88.58(9); C32–Rh–C36, 65.1(1); C33–Rh–C35, 66.6(1).

In this case, the C–H bond of the di(1-naphthyl)methyl group points towards the metal centre and the naphthyl groups arrange themselves in a way which minimises the interactions with the norbornadiene. The C–Rh–N bite angles in the two molecular structures found for the complexes **4d** and **4j** are 77.0(1) and 77.4(1)°, respectively. This reflects the rigidity of this family of oxazolinyl–carbene ligands, which impose a defined geometry upon coordination to a metal centre.

In the ¹H NMR spectra of complexes **4a–j**, recorded at 25 °C, only two signals for the four norbornadiene olefin protons are observed, indicating fast chemical exchange at that temperature. In the light of our previous studies with

achiral oxazolinylicarbene rhodium complexes, the dynamic processes observed in solution are due to a sequence of Berry pseudorotations combined with a fast bromide dissociation and association mechanism.^[5b] The latter equilibrates the two diastereoisomers (derived from the arrangement of the ligands around the rhodium centre) very rapidly in solution and thus leads to average ¹H and ¹³C NMR spectra of the two forms.

While rotation around the C_{Aryl}-N_{Imidazolyl} bond in imidazolium salts **3a-f** is nonhindered and rapid on the NMR timescale at room temperature, complexation to the "RhBr-(nbd)" fragment blocks this rotation for **4c-e** at 25 °C, leading to the observation of, for example, two sets of signals for the *ortho*-methyl (**4c** and **4d**) and isopropyl groups (**4e**; Figure 2).

Complexes **4b** and **4f** possess *ortho*-monosubstituted aryl substituents, which may adopt two inequivalent orientations, thus allowing the existence of two atropisomeric conformers in solution. The two conformers of **4f** (with a bulky *tert*-butyl group as substituent) are present in a ratio of 77:23 at 25 °C. This ratio is obtained under kinetic control during the formation of the complexes and then frozen, since the activation barrier for the interconversion of the conformers is too high to allow their equilibration even at higher temperatures (below the decomposition point of the complex in solution). In contrast, the two atropisomeric forms of **4b** interconvert rapidly on the NMR timescale at 25 °C, leading to a single average signal at $\delta=2.17$ ppm of the *ortho*-methyl group in the two exchanging species (Figure 3). At -5 °C this resonance coalesces and two signals at $\delta=2.38$ and 2.03 ppm are observed at -51 °C. In the slow exchange regime below this temperature the ratio of the two atropisomers corresponds to an apparent equilibrium constant of 1.4.

Hydrosilylation of ketones

Catalyst optimisation: As a reference reaction for the catalyst optimisation we chose the hydrosilylation of acetophe-

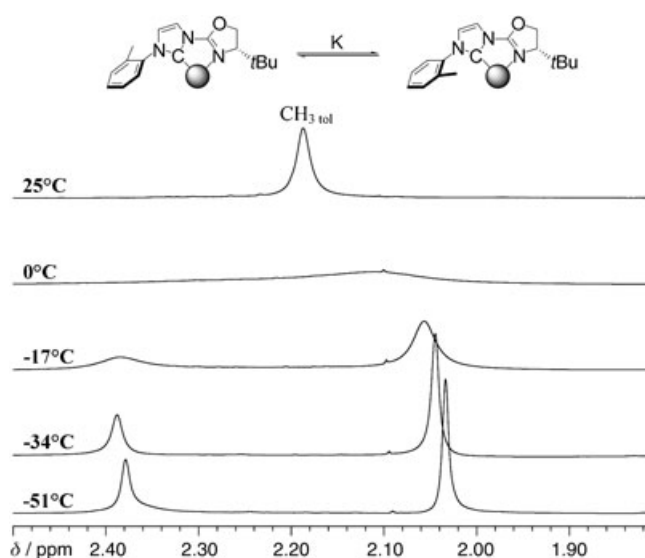


Figure 3. Variable temperature ¹H NMR spectrum of complex **4b** in the region 2.5–1.8 ppm (recorded in CD₂Cl₂, 300 MHz).

none with diphenylsilane at 25 °C. Complexes **4a-j** were used in the presence of AgBF₄ in dichloromethane, giving the active cationic square-planar catalysts. With a catalyst loading of 1.0 mol % at room temperature, satisfactory isolated yields of the secondary alcohol were obtained in all cases (from 70% for the catalytic conversion with complex **4i** to 93% with complex **4j**). Figure 4 summarises the enantioselectivities that were obtained for all complexes under these standardised reaction conditions.

Not unexpectedly, the level of enantioselectivity observed is extremely dependent upon the substituents and there are several notable aspects. Whereas a phenyl substituent on the imidazole ring of the catalyst derived from **4a** gives racemic 1-phenylethanol, the use of the bulkier mesityl substituent (in **4d**) results in an enantiomeric excess of 65%. The use of an aryl group as imidazolidine substituent gives the products with absolute *S* configuration (given the *S* configuration at

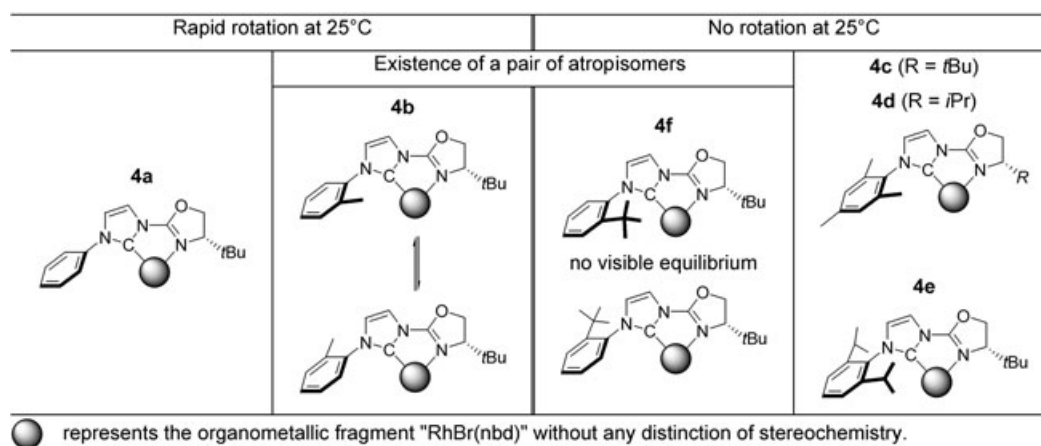


Figure 2. Schematic representation of the influence of the aryl group on the rotation N_{Im}-C_{Ar} in complexes **4a-f**.

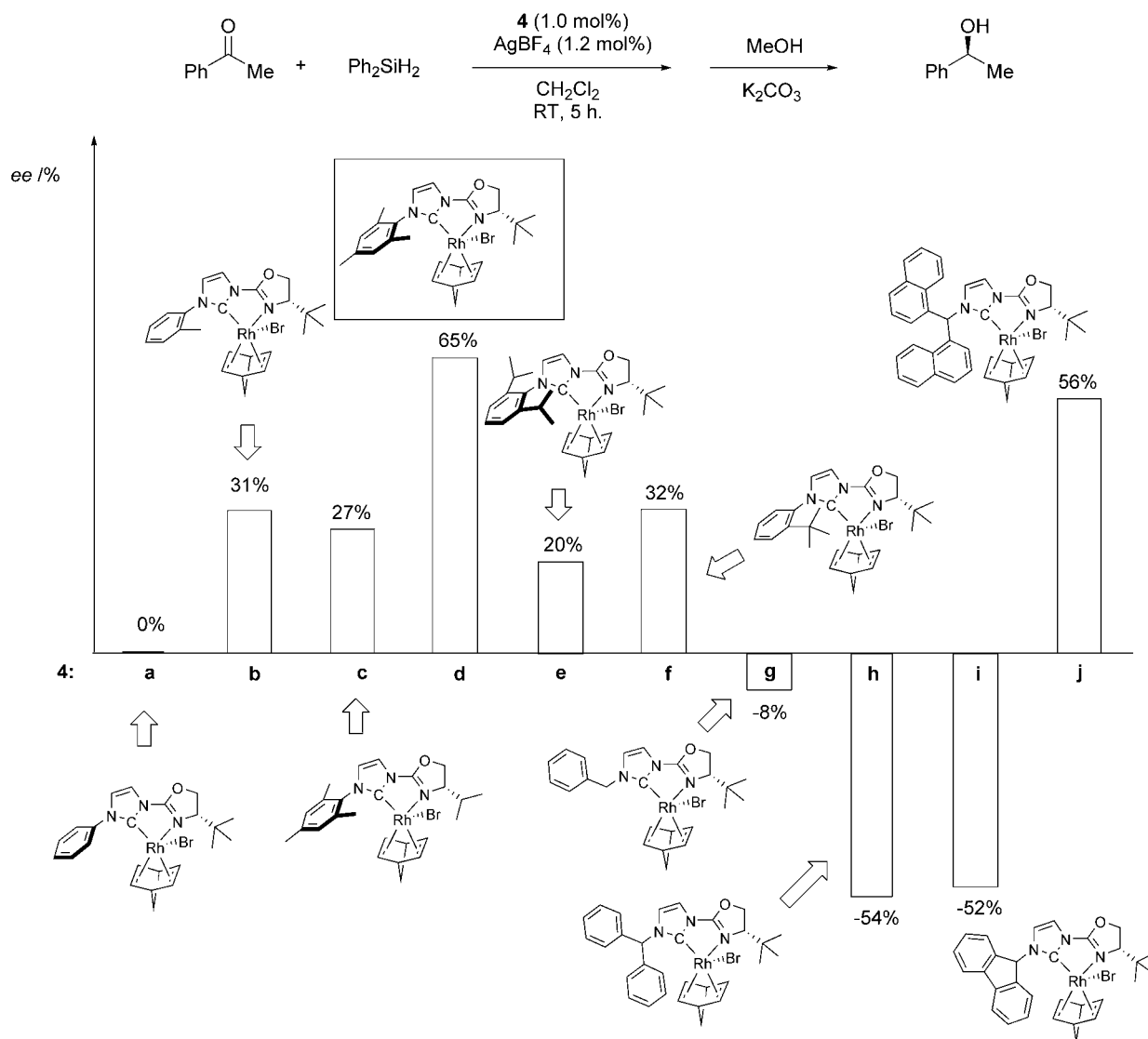


Figure 4. Enantioselectivity data for the hydrosilylation of acetophenone with diphenylsilane with a catalyst loading of 1.0 mol% in the presence of AgBF₄ (experimental conditions: CH₂Cl₂, room temperature, 5 h then hydrolysis with K₂CO₃ in methanol).

the substituent position in the oxazoline units). However, replacement of the aryl by an arylmethyl substituent at the NHC-unit, as in catalysts **4g–i**, the *R* enantiomer was obtained. The only exception to this observation is the derivative with the sterically very demanding di(1-naphthyl)methyl group (**4j**), yielding again the *S*-configured product. Finally, the results obtained with the two oxazolines employed in the ligand assembly established a higher selectivity for the derivatives with the *tert*-butyl groups relative to those with isopropyl substituents in the 4-position of the oxazoline. As a result of this first screening, we selected precatalyst **4d** for further studies of the catalyst performance.

The effect of counterion and the choice of solvent on the catalyst selectivity was investigated for the hydrosilylation of acetophenone by using the cationic catalyst derived from **4d** with a slight excess of various silver salts.^[16] A slight decrease in enantioselectivity is observed in the series BF₄⁻ >

OTs⁻ > BPh₄⁻ > PF₆⁻ > OTf⁻ > B(C₆F₅)₄⁻, whereas CH₂Cl₂ was found to give the best results among various polar solvents that were tested. In several previous studies on asymmetric hydrosilylation catalysis it was found that high enantioselectivity can be afforded by using diarylsilanes that contain sterically demanding aryl groups.^[8c–e,17] In the case at hand, the enantioselectivity was found to be dependent on the choice of the silane (Table 2). On the one hand, methylphenylsilane provided a nearly racemic product (3% *ee*; entry 1), whilst the use of diarylsilanes with greater steric demand than diphenylsilane equally led to a marked decrease in enantioselectivity (entries 4–6). Furthermore, the activity of the catalyst was significantly lower with these sterically crowded silanes.

Temperature dependence of the catalyst selectivity and its implications for the mechanism of stereoselection: Using the

Table 2. Hydrosilylation of acetophenone with catalyst **4d** as a function of the silane.

Entry	Silane	<i>ee</i> [%]
1	MePhSiH ₂	3
2	Ph ₂ SiH ₂	65
3	(<i>p</i> -tol)PhSiH ₂	58
4	(<i>o</i> -tol)PhSiH ₂	-10
5	(α -naphthyl)PhSiH ₂	-7
6	(<i>o</i> -tol) ₂ SiH ₂	-12

optimised catalyst and the reaction conditions identified in the systematic study described above, the temperature dependence of the catalyst performance was determined in the range of -78 to $+25$ °C. Interestingly, we found that the reaction product (1-phenylethanol) is obtained with the highest *ee* by carrying out the reaction at -60 °C, whilst the enantioselectivity drops upon going both to lower and higher temperatures as is shown in Figure 5 (top). As alternative way to represent this result, an Eyring diagram,^[18] plotting $\ln(S/R)$ (S/R =product enantiomer ratio) versus the

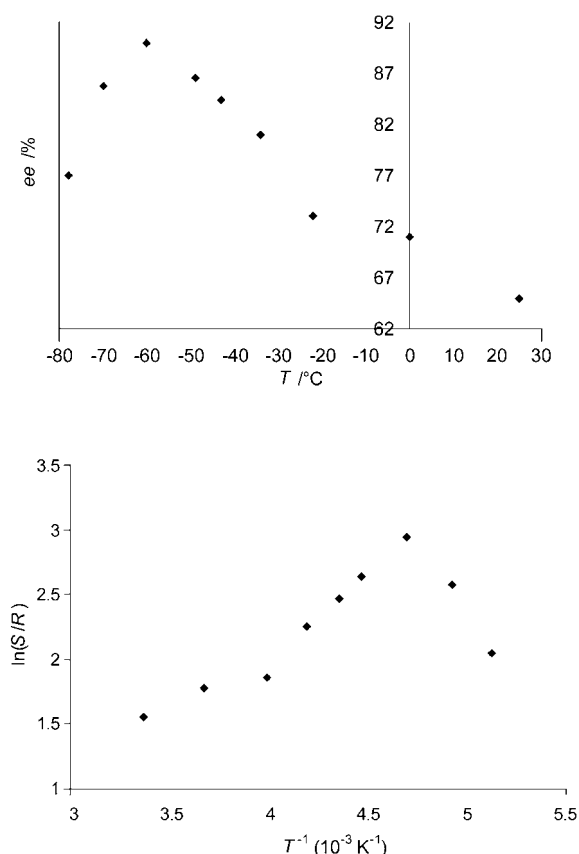
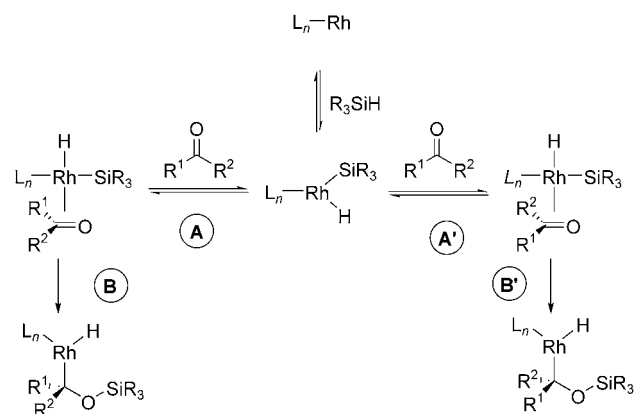


Figure 5. Top: Temperature dependence of the asymmetric hydrosilylation of acetophenone in the presence of system **4d**/AgBF₄ as catalyst (1.0 mol% in CH₂Cl₂) (*ee* vs temperature); Bottom: Eyring diagram ($\ln(S/R)$ vs T^{-1}).

inverse absolute temperature, is displayed alongside (Figure 5, bottom).

If the selectivity determining step had remained the same over the whole temperature range, one would have expected a linear relationship of $\ln(S/R)$ versus T^{-1} and the observation that the temperature dependence of the *ee* values goes through a maximum indicates a change in the selectivity determining step as the temperature is varied. Such behaviour, occasionally referred to as an isoinversion relationship, has been observed inter alia in the asymmetric dihydroxylation of olefins,^[19] the diastereoselective reduction of 2-*tert*-butylcyclohexanone^[20] and the photochemically induced Paterno-Büchi reaction of chiral phenyl glycoalates with cyclic olefins.^[21] Recently, Scharf and co-workers observed such a nonlinear temperature dependence for the enantioselective hydrosilylation of ketones using chiral cyclic monophosphonite rhodium catalysts.^[22]

In a detailed analysis of this phenomenon, Hale and Ridd concluded that the observation of a maximum in a $\ln(S/R)$ versus T^{-1} plot may be taken as evidence for two selectivity determining stages in a reaction.^[23] In our case, the low-temperature slope may be identified with the enthalpic and entropic discrimination involved in that regime ($\Delta\Delta H^\ddagger \approx 15 \text{ kJ mol}^{-1}$, $\Delta\Delta S^\ddagger \approx 96 \text{ J mol}^{-1} \text{ K}^{-1}$), while the region on the side of the maximum towards higher temperature may be viewed as representing a (rather broad) transitional regime with enthalpic and entropic characteristics of a second rate-determining step as the limit. As for hydrosilylation catalysis, the observations are consistent with the mechanistic scheme put forward by Ojima^[24] in which the reversible enantioface differentiating coordination of the ketone to the hydridorhodium complex and the subsequent irreversible insertion of the carbonyl into the Si–Rh bond (Scheme 1) provide two stages at which the stereochemical outcome of the hydrosilylation can be determined.



Scheme 1. Schematic presentation of the two stages (A and B) that determine the stereochemistry of the product.

The determination of the initial reaction rate in the hydrosilylation of acetophenone upon varying the catalyst (**4d**) and substrate concentrations at -55 °C established a

rate law for the initial conversion that is first-order in both substrates as well as the catalyst ($V_i = k[4d][PhCOMe][Ph_2SiH_2]$).^[25]

The first-order dependence on the catalyst concentration was only observed at catalyst loadings below $1.0 \times 10^{-2} \text{ mol L}^{-1}$. At higher catalyst loadings, a marked nonlinear behaviour of the initial rate was observed which was accompanied by a similar concentration profile for the enantiomeric excess (Figure 6). We attribute this behaviour to catalyst aggregation at higher concentrations, accompanied by a change of colour of the reaction solutions from yellow to deep orange upon increasing the concentration of the rhodium catalyst.

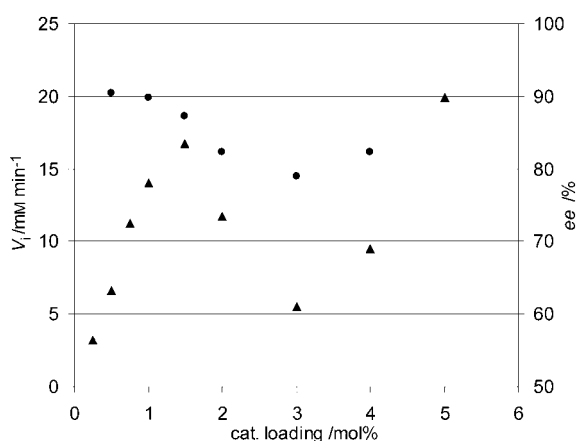


Figure 6. Kinetics of the hydrosilylation of acetophenone at varying concentrations of catalyst (▲) among with the enantiomeric excess of the product (●).

The “proof of the pudding...”—hydrosilylation of ketones with catalyst 4d: The key to the high enantioselectivity observed in the hydrosilylation of ketones with the cationic active catalyst derived from complex **4d** is its remarkably high catalytic activity, which permits its application at the optimised temperature of -60°C with acceptable reaction times and excellent yields. Under these conditions the enantioselectivity is generally good for aryl/alkyl ketones and truly remarkable in the case of the reduction of prochiral dialkyl ketones (vide infra).

Hydrosilylation of aromatic ketones: Under the optimised conditions described above, the cationic catalyst derived from complex **4d** was found to afford high yields and good enantioselectivities in the reduction of various aryl alkyl ketones (Table 3). Acetophenone is reduced in 92% isolated yield and 90% *ee* (entry 1), while 2-naphthyl methyl ketone is isolated in 99% yield with an *ee* of 91% (entry 2). We found that *ortho*-substitution of the aryl substituent resulted in lower enantioselectivities (entries 3, 4) and a similar trend is observed for substrates with bulkier alkyl groups at the CO unit (entry 5). Various derivatives with electronically different substituents have been investigated for which *ee*'s

Table 3. Catalytic asymmetric hydrosilylation of aryl alkyl ketones with catalyst **4d**.

Entry	Ketone	<i>ee</i> [%] ^[a]	Yield [%]
1		90	92
2		91	99
3		75	90
4		86	82
5		70	94
6		88	92
7		91	90
8		78	88
9		85	84
10		81	80
11		89	93

between 78 and 91% were found (entries 6–9), while cyclic aromatic ketones were reduced with equally good enantioselectivity (entries 10, 11).

Hydrosilylation of dialkyl ketones: For the hydrosilylation of dialkyl ketones it has previously proved to be more difficult to obtain high enantioselectivity.^[8] Table 4 summarises the results obtained with various nonaromatic ketones in the presence of catalytic system derived from **4d** and the optimised experimental conditions. Whereas cyclopropyl methyl ketone is hydrosilylated with an enantioselectivity of 81% *ee* (entry 1),^[26] the increase of the steric demand of one of the alkyl groups leads to improved *ee*'s, reaching 95% *ee* in the case of *tert*-butyl methyl ketone (entries 1–4). Linear chain *n*-alkyl methyl ketones, which are particularly challenging substrates, are reduced in good asymmetric in-

Table 4. Catalytic asymmetric hydrosilylation of dialkyl ketones with catalyst **4d**.

Entry	Ketone	ee [%]	Yield [%]
1		81	63 ^[a]
2		88	53 ^[a]
3		89	98
4		95	70 ^[a]
5		77	97
6		79	95
7		74	88 ^[b]
8		65	n.d. ^[b]

[a] Moderate yield due to the volatility of the product. [b] Reaction carried out at -40°C .

duction (entries 5–8), such as 2-octanone (95% isolated yield, 79% ee, entry 6) and even for the extreme case of 2-butanone (65% ee, entry 8).^[27] The results displayed in Table 4 are comparable or even superior to the best previously reported for prochiral nonaromatic ketones.^[8d,28]

Conclusion

In this work we have devised a successful *search strategy* for a new class of rhodium-based highly stereoselective hydrosilylation catalysts. By choice of a modular catalyst design the rapid identification of a system with excellent catalytic activity and enantioselectivity was achieved. The process of optimisation revealed in particular a complex dependence of the catalyst performance on the temperature and the catalyst loading. This is, inter alia, indicative of mechanistic complexity of the system which defies a preconceived “design” approach in its true sense. In view of the simplicity of the ligand and catalyst assembly, the combination of similar building blocks for the development of catalysts for other organic transformations appears to be promising. Such work is currently under way.

Experimental Section

All manipulations were performed under an inert atmosphere of dry nitrogen by using standard Schlenk techniques or by working in a glove box. THF and diethyl ether were distilled from sodium/benzophenone. Pentane was distilled from a sodium/potassium alloy, dichloromethane was dried over CaH_2 and subsequently distilled. ^1H and ^{13}C NMR spectra were recorded on a Bruker Avance 300 NMR spectrometer at 300 MHz and 75 MHz and were referenced using the residual proton solvent peak (^1H) or carbon resonance (^{13}C). Infrared spectra were obtained on a FT-IR Perkin Elmer 1600 spectrometer and the mass spectra were recorded by the “service de spectrométrie de masse de l’Université Louis Pasteur” on an Autospec HF mass spectrometer. The elemental analyses were performed by the analytical services of the Strasbourg and Heidelberg Chemistry Departments. $[\{\text{RhCl}(\text{nbd})\}_2]$ was prepared according to a literature procedure.^[27] (1-Naphth)PhSiH₂ and (*o*-Tol)PhSiH₂ were prepared by reaction of (1-Naphth)MgBr or (*o*-Tol)MgBr with PhSiCl₃ in THF and further reduction with LiAlH₄ in the same flask.^[28] (*o*-Tol)₂SiH₂ was prepared by using HSiCl₃ as the starting chlorosilane. Potassium *tert*-butoxide was sublimed prior to use. RhCl₃·3H₂O was provided by BASF AG (Ludwigshafen) and *tert*-leucine by Degussa AG. All other reagents were commercially available and used as received.

Preparation of the ligands

(4S)-2-Bromo-4-isopropylloxazoline (1a): *t*BuLi (21.7 mL, 1.7 M in pentane, 36.8 mmol) was added dropwise to a solution of (4S)-4-isopropylloxazoline (3.79 g, 33.5 mmol) in anhydrous THF (100 mL) at -78°C over 5 min. The resulting yellow solution was then stirred for an additional 15 min prior to the addition of 1,2-dibromo-1,1,2,2-tetrafluoroethane (4.84 mL, 36.8 mmol). The solution was then allowed to warm to ambient temperature overnight, and was concentrated to about 15 mL. The brownish mixture was purified by a short bulb-to-bulb distillation to yield a colorless solution of the expected bromooxazoline in THF (concentration of about 77% w/w) (4.6 g, 55%). ^1H NMR (CDCl_3): δ = 4.45 (dd, J = 8.3, 9.7 Hz, 1H; CH_2), 4.15 (pseudo-t, J = 8.2 Hz, 1H; CH_2), 3.96 (m, 1H; CH_{oxa}), 1.80 (m, 1H; $\text{CH}(\text{CH}_3)$), 0.99 (d, J = 6.7 Hz, 3H; $\text{CH}(\text{CH}_3)_2$), 0.91 ppm (d, J = 6.7 Hz, 3H; $\text{CH}(\text{CH}_3)_2$); ^{13}C [^1H] NMR (CDCl_3): δ = 141.7 (NCO), 73.2 ($\text{CH}_{2\text{oxa}}$), 72.9 (CH_{oxa}), 32.5 ($\text{CH}(\text{CH}_3)_2$), 18.4, 18.1 ppm ($\text{CH}(\text{CH}_3)_2$).

(4S)-2-Bromo-4-*tert*-butyloxazoline (1b): *t*BuLi (10.8 mL, 1.7 M in pentane, 18.3 mmol) was added dropwise to a solution of (4S)-4-*tert*-butyloxazoline (2.11 g, 16.6 mmol) in anhydrous THF (50 mL) at -78°C over 5 min. The resulting yellow solution was then stirred for an additional 15 min prior to the addition of 1,2-dibromo-1,1,2,2-tetrafluoroethane (2.4 mL, 18.3 mmol). The solution was then allowed to warm to ambient temperature overnight, and was concentrated to about 5 mL. The light brownish mixture was purified by a short bulb-to-bulb distillation to yield a colorless solution of the expected bromooxazoline in THF (concentration of about 88% w/w) (2.25 g, 66%). ^1H NMR (CDCl_3): δ = 4.38 (dd, J = 8.4, 10.0 Hz, 1H; CH_2), 4.24 (dd, J = 8.0, 8.4 Hz, 1H; CH_2), 3.92 (dd, J = 8.0, 10.0 Hz, 1H; CH_{oxa}), 0.92 ppm (s, 9H; $\text{C}(\text{CH}_3)_3$); ^{13}C [^1H] NMR (CDCl_3): δ = 141.4 (NCO), 76.3 (CH), 71.6 (CH_2), 35.6 ($\text{C}(\text{CH}_3)_3$), 25.5 ppm ($\text{C}(\text{CH}_3)_3$).

Imidazolium salts—general procedure: The imidazole (1–5 mmol) was added to a concentrated solution of the bromooxazoline (1.15 equiv) in THF ($c > 2\text{M}$) and the solution was stirred during 2–5 days at ambient temperature. During the course of this period, the mixture became solid and had to be crushed with a spatula. The colourless solid was washed several times with Et₂O (2 mL mmol⁻¹) and dried in vacuo.

1-[(5S)-4-*tert*-Butyl-4,5-dihydrooxazol-2-yl]-3-phenylimidazolium bromide (3a): Yield 70%; ^1H NMR (CDCl_3): δ = 10.47 (pseudo-t, 4J = 1.6 Hz, 1H; NCHN), 8.38 (dd, 3J = 2.1 Hz, 4J = 1.6 Hz, 1H; $\text{CH}_{4/5\text{-Im}}$), 8.04 (m, 2H; CH_{Ph}), 7.97 (dd, 3J = 2.1 Hz, 4J = 1.6 Hz, 1H; $\text{CH}_{4/5\text{-Im}}$), 7.50 (m, 3H; CH_{Ph}), 4.74 (dd, 2J = 8.8 Hz, 3J = 9.8 Hz, 1H; $\text{CH}_{2\text{oxa}}$), 4.54 (pseudo-t, J = 8.6 Hz, 1H; $\text{CH}_{2\text{oxa}}$), 4.12 (dd, 3J = 8.5 Hz, 3J = 9.8 Hz, 1H; CH_{oxa}), 0.9 ppm (s, 9H; $\text{C}(\text{CH}_3)_3$); ^{13}C [^1H] NMR (CDCl_3): δ = 149.3 (NCO), 135.0, 133.9 (N₂C, C_{Ph}), 131.0 (CH_{Ph}), 130.5 (CH_{Ph}), 123.6 (CH_{Im}), 122.9 (CH_{Ph}), 120.8 (CH_{Im}), 75.1 (CH_{oxa}), 73.1 ($\text{CH}_{2\text{oxa}}$), 33.9 ($\text{C}(\text{CH}_3)_3$),

24.9 ppm (C(CH₃)₃); MS (FAB): *m/z* (%): 270 (100) [M⁺-Br]; FT-IR (KBr): $\tilde{\nu}$ =1694 cm⁻¹ (s, C=N); elemental analysis calcd (%) for C₁₆H₂₀BrN₃O (350.26): C 54.87, H 5.76, N 12.00; found: C 54.67, H 5.64, N 11.93.

1-[(S)-4-*tert*-Butyl-4,5-dihydrooxazol-2-yl]-3-(2-tolyl)imidazolium bromide (3b): Yield 84%; ¹H NMR (CDCl₃): δ =10.03 (pseudo-t, ⁴J=1.6 Hz, 1H; NCHN), 8.06 (dd, ³J=2.1 Hz, ⁴J=1.6 Hz, 1H; CH_{4/5-Im}), 7.94 (dd, ³J=2.1 Hz, ⁴J=1.6 Hz, 1H; CH_{4/5-Im}), 7.82 (m, 1H; CH_{tol}), 7.44–7.26 (m, 3H; CH_{tol}), 4.73 (dd, ²J=8.7 Hz, ³J=9.9 Hz, 1H; CH_{2oxa}), 4.54 (pseudo-t, J=8.6 Hz, 1H; CH_{2oxa}), 4.12 (dd, ³J=8.5 Hz, ³J=9.8 Hz, 1H; CH_{oxa}), 2.31 (s, 3H; CH_{3tol}), 0.96 ppm (s, 9H; C(CH₃)₃); ¹³C {¹H} NMR (CDCl₃): δ =149.3 (NCO), 136.7 (N₂C), 133.3 (C_{tol}), 133.2 (C_{tol}), 132.0 (CH_{tol}), 131.6 (CH_{tol}), 127.9 (CH_{tol}), 127.7 (CH_{tol}), 125.8 (CH_{im}), 120.6 (CH_{im}), 75.1 (CH_{oxa}), 73.1 (CH_{2oxa}), 33.9 (C(CH₃)₃), 25.8 (C(CH₃)₃), 18.01 ppm (CH_{3tol}); MS (ESI): *m/z* (%): 284.17 (100) [M⁺-Br], 285.17 (13) [M⁺-Br+H]; FT-IR (KBr): $\tilde{\nu}$ =1696.4 cm⁻¹ (s, C=N).

1-[(S)-4-Isopropyl-4,5-dihydrooxazol-2-yl]-3-mesitylimidazolium bromide (3c): Yield: 80%; ¹H NMR (CDCl₃): δ =10.38 (pseudo-t, ⁴J=1.6 Hz, 1H; NCHN), 8.17 (dd, ³J=2.1 Hz, ⁴J=1.6 Hz, 1H; CH_{4/5-Im}), 7.77 (dd, ²J=2.1 Hz, ⁴J=1.6 Hz, 1H; CH_{4/5-Im}), 6.95 (s, 2H; CH_{mes}), 4.82 (dd, ²J=8.5 Hz, ³J=9.4 Hz, 1H; CH_{2oxa}), 4.47 (pseudo-t, ²J=8.5 Hz, ³J=8.5 Hz, 1H; CH_{2oxa}), 4.12 (m, 1H; CH_{oxa}), 2.28 (s, 3H; CH_{3para}), 2.10 (s, 6H; CH_{3ortho}), 1.85 (m, 1H; CH(CH₃)₂), 1.00 (d, J=6.7 Hz, 3H; CH(CH₃)₂), 0.91 ppm (d, J=6.7 Hz, 3H; CH(CH₃)₂); ¹³C {¹H} NMR (CDCl₃): δ =149.4 (NCO), 141.7 (C_{mes}), 137.3 (N₂C), 134.0 (C_{mes}), 130.1 (C_{mes}), 130.0 (CH_{mes}), 126.0 (CH_{im}), 121.2 (CH_{im}), 75.0 (CH_{2oxa}), 71.9 (CH_{oxa}), 32.7 (CH(CH₃)₂), 21.2 (CH_{3para}), 18.8 (CH(CH₃)₂), 18.5 (CH(CH₃)₂), 18.0 ppm (CH_{3ortho}); MS (ESI): *m/z* (%): 298 (84) [M⁺-Br], 187 (100) [M⁺-Br-C₆H₈NO]; FT-IR (KBr): $\tilde{\nu}$ =1696 cm⁻¹ (s, C=N); elemental analysis calcd (%) for C₁₈H₂₂BrN₃O (378.31): C 57.15, H 6.39, N 11.10; found: C 58.41, H 6.43, N 11.10.

1-[(S)-4-*tert*-Butyl-4,5-dihydrooxazol-2-yl]-3-mesitylimidazolium bromide (3d): Yield: 71% (reaction time: 5 d); ¹H NMR (CDCl₃): δ =10.43 (pseudo-t, ⁴J=1.6 Hz, 1H; NCHN), 8.18 (dd, ³J=2.1 Hz, ⁴J=1.6 Hz, 1H; CH_{4/5-Im}), 7.80 (dd, ³J=2.1 Hz, ⁴J=1.6 Hz, 1H; CH_{4/5-Im}), 6.96 (s, 2H; CH_{mes}), 4.76 (dd, ²J=8.8 Hz, ³J=9.9 Hz, 1H; CH_{2oxa}), 4.55 (pseudo-t, J=8.6 Hz, 1H; CH_{2oxa}), 4.14 (dd, ³J=8.8 Hz, ³J=9.9 Hz, 1H; CH_{oxa}), 2.28 (s, 3H; CH_{3para}), 2.10 (s, 6H; CH_{3ortho}), 0.93 ppm (s, 9H; C(CH₃)₃); ¹³C {¹H} NMR (CDCl₃): δ =149.4 (NCO), 141.8 (C_{mes}), 137.4 (N₂C), 134.0 (C_{mes}), 130.2 (C_{mes}), 130.0 (CH_{mes}), 126.1 (CH_{im}), 121.2 (CH_{im}), 75.2 (CH_{oxa}), 73.1 (CH_{2oxa}), 33.9 (C(CH₃)₃), 25.8 (C(CH₃)₃), 21.1 (CH_{3para}), 18.0 ppm (CH_{3ortho}); MS (ESI): *m/z*: 312.2038 [M⁺-Br]; FT-IR (KBr): $\tilde{\nu}$ =1699 cm⁻¹ (s, C=N); elemental analysis calcd (%) for C₁₉H₂₆BrN₃O (392.34): C 58.17, H 6.68, N 10.71, found: C 57.50, H 6.66, N 10.42.

1-[(S)-4-*tert*-Butyl-4,5-dihydrooxazol-2-yl]-3-(2,6-diisopropylphenyl)imidazolium bromide (3e): Yield: 96% (reaction time 4 d); ¹H NMR (CDCl₃): δ =10.56 (brs, 1H; NCHN), 8.35 (dd, J=2.1 Hz, ⁴J=1.6 Hz, 1H; CH_{4/5-Im}), 7.68 (dd, ³J=2.1 Hz, ⁴J=1.6 Hz, 1H; CH_{4/5-Im}), 7.56 (t, ³J=8.0 Hz, 1H; CH_{Ar}), 7.34 (d, ³J=8.0 Hz, 2H; CH_{Ar}), 4.86 (pseudo-t, J=9.5 Hz, 1H; CH_{2oxa}), 4.65 (pseudo-t, J=8.6 Hz, 1H; CH_{2oxa}), 4.21 (pseudo-t, J=9.5 Hz, 1H; CH_{oxa}), 2.43 (m, 2H; CH(CH₃)₂), 1.29 (d, ³J=6.8 Hz, 6H; CH(CH₃)₂), 1.18 (d, ³J=6.8 Hz, 3H; CH(CH₃)₂), 1.17 (d, ³J=6.8 Hz, 3H; CH(CH₃)₂), 0.99 ppm (s, 9H; C(CH₃)₃); ¹³C {¹H} NMR (CDCl₃): δ =149.3 (NCO), 141.0, 137.7, 132.4 (C_{Ar}, N₂C), 126.5 (CH_{Ar}), 124.9 (CH_{im}), 121.2 (CH_{im}), 75.2 (CH_{oxa}), 73.4 (CH_{2oxa}), 33.8 (C(CH₃)₃), 28.9 (CH(CH₃)₂), 25.9 (C(CH₃)₃), 24.5 (CH(CH₃)₂), 24.2 (CH(CH₃)₂); MS (ESI): *m/z* (%): 354.25 (100) [M⁺-Br], 355.25 (22) [M⁺-Br+H]; FT-IR (KBr): $\tilde{\nu}$ =1692.7 cm⁻¹ (s, C=N).

1-[(S)-4-*tert*-Butyl-4,5-dihydrooxazol-2-yl]-3-(2-*tert*-butylphenyl)imidazolium bromide (3f): Yield: 70%; ¹H NMR (CDCl₃): δ =9.84 (brs, 1H; NCHN), 8.10 (dd, ³J=2.1 Hz, ⁴J=1.6 Hz, 1H; CH_{4/5-Im}), 7.92 (m, 1H; CH_{Ar}), 7.71 (dd, ³J=2.1 Hz, ⁴J=1.6 Hz, 1H; CH_{4/5-Im}), 7.61 (m, 1H; CH_{Ar}), 7.54 (m, 1H; CH_{Ar}), 7.39 (m, 1H; CH_{Ar}), 4.77 (pseudo-t, J=9.2 Hz, 1H; CH_{2oxa}), 4.59 (pseudo-t, J=8.6 Hz, 1H; CH_{2oxa}), 4.18 (dd, ³J=8.7 Hz, ³J=9.8 Hz, 1H; CH_{oxa}), 1.24 (s, 9H; C(CH₃)_{3ortho}), 0.96 ppm (s, 9H; C(CH₃)_{3oxa}); ¹³C {¹H} NMR (CDCl₃): δ =149.2 (NCO), 145.3 (C_{Ar}), 137.9 (N₂C), 132.2 (C_{Ar}), 132.0, 130.6, 128.7, 128.1 (CH_{Ar}), 127.2 (CH_{im}), 120.0 (CH_{im}), 75.2 (CH_{oxa}), 73.1 (CH_{2oxa}), 35.9 (C(CH₃)_{3ortho}), 33.9

(C(CH₃)_{3oxa}), 32.0 (C(CH₃)_{3ortho}), 25.8 ppm (C(CH₃)_{3oxa}); MS (ESI): *m/z* (%): 326.22 (100) [M⁺-Br], 327.22 (22) [M⁺-Br+H]; FT-IR (KBr): $\tilde{\nu}$ =1695.1 cm⁻¹ (s, C=N).

1-[(S)-4-*tert*-Butyl-4,5-dihydrooxazol-2-yl]-3-benzylimidazolium bromide (3g): Yield: 91%; ¹H NMR (CDCl₃): δ =10.91 (brs, 1H; NCHN), 7.78 (brs, 1H; CH_{4/5-Im}), 7.71–7.66 (m, 3H; CH_{4/5-Im}, 2CH_{Ph}), 7.38–7.35 (m, 3H; CH_{Ph}), 6.05 (s, 2H; CH_{2Ph}), 4.67 (dd, ²J=8.9 Hz, ³J=9.8 Hz, 1H; CH_{2oxa}), 4.47 (pseudo-t, J=8.7 Hz, 1H; CH_{2oxa}), 4.08 (dd, ³J=8.6 Hz, ³J=9.8 Hz, 1H; CH_{oxa}), 0.90 ppm (s, 9H; C(CH₃)₃); ¹³C {¹H} NMR (CDCl₃): δ =149.2 (NCO), 136.7 (N₂C), 132.7 (C_{Ph}), 129.7 (CH_{Ph}), 129.7 (CH_{Ph}), 129.5 (CH_{Ph}), 123.6 (CH_{im}), 119.5 (CH_{im}), 75.0 (CH_{oxa}), 73.0 (CH_{2oxa}), 54.0 (CH_{2Ph}), 33.8 (C(CH₃)₃), 25.6 ppm (C(CH₃)₃); MS (ESI): *m/z* (%): 284.16 (100) [M⁺-Br], 285.17 (16) [M⁺-Br+H]; FT-IR (KBr): $\tilde{\nu}$ =1699 cm⁻¹ (s, C=N).

1-[(S)-4-*tert*-Butyl-4,5-dihydrooxazol-2-yl]-3-(diphenylmethyl)imidazolium bromide (3h): Yield: 86%; ¹H NMR (CDCl₃): δ =10.73 (brs, 1H; NCHN), 8.43 (s, 1H; CHPh₂), 7.80 (t, J=1.9 Hz, 1H; CH_{4/5-Im}), 7.43–7.37 (m, 10H; CH_{Ph}), 7.35 (pseudo-t, J=1.75 Hz, 1H; CH_{4/5-Im}), 4.70 (dd, ²J=9.0 Hz, ³J=9.8 Hz, 1H; CH_{2oxa}), 4.52 (pseudo-t, J=8.8 Hz, 1H; CH_{2oxa}), 4.11 (dd, ³J=8.7 Hz, ³J=9.8 Hz, 1H; CH_{oxa}), 0.94 ppm (s, 9H; C(CH₃)₃); ¹³C {¹H} NMR (CDCl₃): δ =149.2 (NCO), 137.5 (N₂C), 135.9 (C_{Ph}), 129.5, 129.4, 128.6 (CH_{Ph}), 122.7 (CH_{im}), 119.3 (CH_{im}), 75.1 (CH_{oxa}), 73.1 (CH_{2oxa}), 67.0 (CHPh₂), 33.9 (C(CH₃)₃), 25.7 ppm (C(CH₃)₃); MS (ESI): *m/z* (%): 360.22 (100) [M⁺-Br], 361.22 (85) [M⁺-Br+H]; FT-IR (KBr): $\tilde{\nu}$ =1698 cm⁻¹ (s, C=N); elemental analysis calcd (%) for C₂₅H₂₆BrN₃O (440.38): C 62.73, H 5.95, N 9.54; found: C 62.52, H 5.93, N 9.48.

1-[(S)-4-*tert*-Butyl-4,5-dihydrooxazol-2-yl]-3-fluorenylimidazolium bromide (3i): Yield: 92%; ¹H NMR (CDCl₃): δ =11.86 (brs, 1H; NCHN), 7.92 (brs, 1H; CH_{4/5-Im}), 7.76–7.67 (m, 5H; CH_{4/5-Im}, 4CH_{fluor}), 7.49–7.33 (m, 4H; CH_{fluor}), 4.72 (dd, J=9.1, 9.7 Hz, 1H; CH_{2oxa}), 4.55 (pseudo-t, J=8.8 Hz, 1H; CH_{2oxa}), 4.12 (dd, ³J=8.7 Hz, ³J=9.8 Hz, 1H; CH_{oxa}), 0.94 ppm (s, 9H; C(CH₃)₃); ¹³C {¹H} NMR (CDCl₃): δ =149.3 (NCO), 141.0, 139.3, 138.4 (N₂C, C_{fluor}, C_{fluor}), 130.7, 128.8, 126.2 (CH_{fluor}), 120.9 (CH_{im}), 120.7 (CH_{fluor}), 119.7 (CH_{im}), 75.0 (CH_{oxa}), 73.1 (CH_{2oxa}), 63.6 (CH_{2-fluor}), 33.9 (C(CH₃)₃), 25.7 ppm (C(CH₃)₃); MS (ESI): *m/z* (%): 358.19 (100) [M⁺-Br], 359.19 (18) [M⁺-Br+H]; FT-IR (KBr): $\tilde{\nu}$ =1699 cm⁻¹ (s, C=N); elemental analysis calcd (%) for C₂₅H₂₆BrN₃O (438.37): C 63.02, H 5.52, N 9.58; found: C 63.50, H 5.80, N 9.30.

1-[(S)-4-*tert*-Butyl-4,5-dihydrooxazol-2-yl]-3-[di(α -naphthyl)methyl]imidazolium bromide (3j): Yield: 97%; ¹H NMR (CDCl₃): δ =11.16 (s, 1H; NCHN), 9.65 (s, 1H; CHNp₂), 8.49–8.39 (m, 2H; CH_{Np}), 7.93–7.87 (m, 4H; CH_{Np}), 7.77 (brs, 1H; CH_{4/5-Im}), 7.57–7.50 (m, 4H; CH_{Np}), 7.36–7.26 (m, 3H; CH_{4/5-Im}, 2CH_{Np}), 6.92–6.89 (m, 2H; CH_{Np}), 4.67 (dd, ²J=9.0 Hz, ³J=9.8 Hz, 1H; CH_{2oxa}), 4.50 (pseudo-t, J=8.8 Hz, 1H; CH_{2oxa}), 4.10 (dd, ³J=8.7 Hz, ³J=9.8 Hz, 1H; CH_{oxa}), 0.93 ppm (s, 9H; C(CH₃)₃); ¹³C {¹H} NMR (CDCl₃): δ =149.2 (NCO), 138.0 (N₂C), 134.1, 132.5, 132.4 (C_{Np}), 130.7, 128.7, 128.3, 125.9, 124.8, 124.3, 124.2 (CH_{Np}), 123.6 (CH_{im}), 118.9 (CH_{im}), 75.1 (CH_{oxa}), 73.1 (CH_{2oxa}), 62.5 (CHNp₂), 33.8 (C(CH₃)₃), 25.7 ppm (C(CH₃)₃); MS (ESI): *m/z* (%): 267.10 (37) [Np₂CH]⁺, 460.22 (100) [M⁺-Br].

Preparation of the complexes—general procedure: [[RhCl(nbd)]₂] (0.25 mmol) and 2.2 equivalents of potassium *tert*-butoxide were placed in a Schlenk tube. THF was added by syringe so that the solution was 0.02 M with respect to the Rh precursor. After stirring for 30 minutes at ambient temperature, the mixture was slowly added to a suspension of 2.0 equivalents of the imidazolium salt in THF (0.02 M with respect to the imidazolium salt) at -78 °C. The mixture was allowed to warm to ambient temperature overnight and was centrifuged. The supernatant solution was separated and the volatiles were removed in vacuo. The crude solid was washed two or three times with pentane (15 mL mmol⁻¹) and dried.

Bromo-(η^4 -2,5-norbornadiene)-{1-[(S)-4-*tert*-butyl-4,5-dihydrooxazol-2-yl]-3-phenylimidazol-2-ylidene}rhodium(II) (4a): Yield: 87%; ¹H NMR (CDCl₃): δ =8.03 (m, 2H; CH_{Ph}), 7.56–7.46 (m, 3H; CH_{Ph}), 7.33 (d, ³J=2.1 Hz, 1H; CH_{4/5-Im}), 6.97 (d, ³J=2.1 Hz, 1H; CH_{4/5-Im}), 4.78 (dd, ²J=8.7 Hz, ³J=9.7 Hz, 1H; CH_{2oxa}), 4.65 (dd, ²J=8.6 Hz, ³J=7.3 Hz, 1H; CH_{2oxa}), 4.25 (dd, ³J=7.3 Hz, ³J=9.8 Hz, 1H; CH_{oxa}), 3.58 (brs, 2H; CH_{2/3/5/6-nbd}), 3.49 (brs, 2H; CH_{2/3/5/6-nbd}), 3.42 (brs, 2H; CH_{1/4-nbd}), 1.02 (s, 9H; C(CH₃)₃), 1.00 ppm (s, 2H; CH_{2nbd}); ¹³C {¹H} NMR (CDCl₃): δ =

(pseudo-t, $J=7.8$ Hz, 1H; $CH_{2\text{oxa}}$), 4.19 (dd, $^3J=7.8$ Hz, $^3J=9.8$ Hz, 1H; CH_{oxa}), 3.5–3.3 (br, 4H; $CH_{2/3/5/6\text{-nbd}}$), 3.00 (brs, 2H; $CH_{1/4\text{-nbd}}$), 1.00 (s, 9H; $C(CH_3)_3$), 0.74 ppm (s, 2H; $CH_{2\text{nbd}}$); ^{13}C { 1H } NMR ($CDCl_3$): δ = 155.3 (NCO), 133.9, 133.8, 131.4, 130.8 (C_{Np}), 129.8, 129.2, 128.5, 128.2, 127.3, 126.8, 126.4, 125.7, 125.3, 125.0, 124.7, 121.4 (CH_{Np}), 127.8 (CH_{im}), 123.6 (CH_{im}), 74.9 (CH_{oxa}), 72.7 ($CH_{2\text{oxa}}$), 61.9 ($CHNp_2$), 60.8 ($CH_{2\text{nbd}}$), 49.0 ($CH_{1/4\text{-nbd}}$), 34.2 ($C(CH_3)_3$), 25.6 ppm ($C(CH_3)_3$); MS (ESI): m/z (%): 562.13 (11) [$M^+-Br-nbd$], 654.20 (100) [M^+-Br]; FT-IR (KBr): $\tilde{\nu}$ = 1671.2 cm^{-1} (s, C=N).

General procedure for the hydrosilylation catalysis: In a small Schlenk tube, an orange solution of complex **4d** (17.6 mg, 0.030 mmol) in CH_2Cl_2 (0.6 mL) was added to $AgBF_4$ (7.0 mg, 0.012 mmol). The resulting mixture was stirred for about 5 min and then filtered through a pad of Celite and rinsed with an additional of CH_2Cl_2 (0.3 mL). The red solution was divided into three equal parts (for three different catalytic runs; 0.3 mL each) and each vial was topped up to 0.5 mL. After addition of the desired ketone (1.0 mmol) at ambient temperature, the reaction mixture was cooled to $-60^\circ C$ and diphenylsilane (210 μL , 1.1 mmol) was added dropwise over a period of 2 min. The bright yellow reaction mixture was stirred at $-60^\circ C$ for 10 h. A solution of K_2CO_3 in methanol (0.1%, 2.0 mL) was then added and the resulting mixture was stirred for at least 4 h at room temperature. After evaporation of the solvents, the product was purified by column chromatography (2×10 cm, SiO_2 , pentane/ Et_2O : 85/15). Yields refer to isolated yields of compounds estimated to be >95% pure as determined by 1H NMR spectroscopy. Yields and *ee*'s are the average of at least two corroborating runs. Absolute configurations of enantiomerically enriched alcohols were determined by comparing the sign of their optical activities with those reported in literature.

Kinetic studies: Hydrosilylation studies were carried out at $-55^\circ C$ in CD_2Cl_2 as solvent. Each experiment was conducted with freshly prepared rhodium catalyst by reacting complex **4d** with $AgBF_4$ in CD_2Cl_2 followed by filtration through Celite. The solution was then transferred into a NMR tube with the desired amount of acetophenone. In all cases, the sample was allowed to stand at $-55^\circ C$ before adding the diphenyl silane. The progress of the reaction was monitored by measuring the disappearance of the ketone and appearance of the product by 1H NMR spectroscopy.

Crystal structure determinations: Suitable crystals of the complexes **4d** and **4j** were obtained by layering concentrated solutions of the samples in dichloromethane with pentane and allowing slow diffusion at room temperature. Intensity data were collected at low temperature on Nonius Kappa CCD (complex **4d**) and Bruker Smart 1000 CCD (complex **4j**) diffractometers. The radiation used was graphite-monochromated $MoK\alpha$ ($\lambda=0.71073$ Å). A semi-empirical absorption correction was applied. The structures were solved by using direct methods and refined by full-matrix least-squares methods. For complex **4d**, hydrogen atom positions were taken from difference Fourier maps; they were introduced as fixed contributors in the structure factor calculations with fixed coordinates (C–H: 0.95 Å) and isotropic temperature factors ($B(H)=1.3 B_{\text{eq}}(C)$ Å²), but not refined. For complex **4j**, hydrogen atoms were input at calculated positions except for the olefinic hydrogens of the norbornadiene ligand, which were taken from Fourier maps and refined with the C–H distance constrained to 0.95 Å. The calculations were performed by using the programs OpenMoleN,^[31] SHELXS-86^[32] and SHELXL-97.^[33] Graphical representations were drawn with PLATON.^[34] Crystal data and experimental details are given in Table 5.

CCDC 221154 and 262660 contain the supplementary crystallographic data for this paper. These data can be obtained free of charge from The Cambridge Crystallographic Data Centre via www.ccdc.cam.ac.uk/data_request/cif.

Acknowledgements

We thank the CNRS (France) and the Institut Universitaire de France for support of this work and the Ministère de l'Éducation Nationale de la Recherche et de la Technologie for a Ph.D. grant to V.C. Support by

Table 5. X-ray experimental data for compounds **4d** and **4j**.

	4d	4j
formula	$C_{26}H_{33}BrN_3ORh$	$C_{28}H_{37}BrN_3ORh \cdot CH_2Cl_2$
M_r	586.39	819.45
crystal system	orthorhombic	monoclinic
space group	$P2_12_12_1$	$P2_1$
a [Å]	9.7117(1)	12.5400(5)
b [Å]	13.7354(2)	11.4205(5)
c [Å]	18.3991(2)	13.4866(6)
β [°]	90	116.8570(10)
V [Å ³]	2454.33(5)	1723.1(1)
Z	4	2
colour	orange	orange
crystal size [mm]	$0.25 \times 0.20 \times 0.20$	$0.25 \times 0.18 \times 0.08$
ρ_{calcd} [$g\ cm^{-3}$]	1.59	1.579
$F(000)$	1192	832
μ [mm^{-1}]	2.347	1.847
T [K]	173	100
2θ range [°]	5–60	4–64
index range	$-13 \leq h \leq 13$ $-19 \leq k \leq 19$ $-25 \leq l \leq 25$	$-18 \leq h \leq 16$ $-14 \leq k \leq 17$ $0 \leq l \leq 20$
reflins measured	7139	10567
observed reflins	3461	9533
	$I > 3\sigma(I)$	$I > 2\sigma(I)$
parameters	289	443
R (obsvd data)	0.030	0.038
wR	0.048	
$wR2$ (all data)		0.091
Flack parameter	0.01(1)	0.001(6)
GOOF	1.020	1.033
largest difference peak [$e\ \text{Å}^{-3}$]	0.532	1.206

BASF (Ludwigshafen) and Degussa (Hanau) is gratefully acknowledged. We also thank Dr A. De Cian and N. Gruber for the X-ray diffraction studies.

- [1] A. H. Hoveyda, A. W. Hird, M. A. Kaprzynski, *Chem. Commun.* **2004**, 1779.
- [2] Reviews: a) W. A. Herrmann, *Angew. Chem.* **2002**, *114*, 1342; *Angew. Chem. Int. Ed.* **2002**, *41*, 1290; b) D. Bourissou, O. Guerret, F. Gabbai, G. Bertrand, *Chem. Rev.* **2000**, *100*, 39; c) W. A. Herrmann, C. Köcher, *Angew. Chem.* **1997**, *109*, 2257; *Angew. Chem. Int. Ed. Engl.* **1997**, *36*, 2162.
- [3] a) J. A. Chamizo, P. B. Hitchcock, H. A. Jasim, M. F. Lappert, *J. Organomet. Chem.* **1993**, *451*, 89; b) W. A. Herrmann, C. Köcher, L. J. Goossen, G. R. J. Artus, *Chem. Eur. J.* **1996**, *2*, 1627; c) D. S. McGuinness, K. J. Cavell, *Organometallics* **2000**, *19*, 741; d) C. Yang, H. M. Lee, S. P. Nolan, *Org. Lett.* **2001**, *3*, 1511; e) P. L. Arnold, A. C. Scarisbrick, A. J. Blake, C. Wilson, *Chem. Commun.* **2001**, 2340; f) A. A. Danopoulos, S. Winston, T. Gelbrich, M. B. Hursthouse, R. P. Tooze, *Chem. Commun.* **2002**, 482; g) A. A. Danopoulos, S. Winston, M. B. Hursthouse, *J. Chem. Soc. Dalton Trans.* **2002**, 3090; h) P. L. Arnold, *Heteroat. Chem.* **2002**, *13*, 534.
- [4] a) W. A. Herrmann, L. J. Goossen, M. Spiegler, *Organometallics* **1998**, *17*, 2162; b) J. C. C. Chen, I. J. B. Lin, *Organometallics* **2000**, *19*, 5113; c) A. A. D. Tulloch, A. A. Danopoulos, R. P. Tooze, S. M. Cafferkey, S. Kleinhenz, M. B. Hursthouse, *Chem. Commun.* **2000**, 1247; d) E. Peris, J. A. Loch, J. Mata, R. H. Crabtree, *Chem. Commun.* **2001**, 201; e) S. Gründemann, A. Kovacevic, M. Albrecht, J. W. Faller, R. H. Crabtree, *Chem. Commun.* **2001**, 2274; f) S. Gründemann, M. Albrecht, J. A. Loch, J. W. Faller, R. H. Crabtree, *Organometallics* **2001**, *20*, 5485; g) A. A. D. Tulloch, A. A. Danopoulos, G. J. Tizzard, S. J. Coles, M. B. Hursthouse, R. S. Hay-Motherwell, W. B. Motherwell, *Chem. Commun.* **2001**, 1270; h) S. Gründemann,

- A. Kovacevic, M. Albrecht, J. W. Faller, R. H. Crabtree, *J. Am. Chem. Soc.* **2002**, *124*, 10473; i) A. A. Danopoulos, S. Winston, W. B. Motherwell, *Chem. Commun.* **2002**, 1376; j) J. A. Loch, M. Albrecht, E. Peris, J. Mata, J. W. Faller, R. H. Crabtree, *Organometallics* **2002**, *21*, 700; k) J. J. Van Veldhuizen, S. B. Garber, J. S. Kingsbury, A. H. Hoveyda, *J. Am. Chem. Soc.* **2002**, *124*, 4954; l) A. A. Danopoulos, S. Winston, M. B. Hursthouse, *J. Chem. Soc. Dalton Trans.* **2002**, 3090; m) A. A. D. Tulloch, S. Winston, A. A. Danopoulos, G. Eastham, M. B. Hursthouse, *Dalton Trans.* **2003**, 699; n) M. C. Perry, X. Cui, M. T. Powell, D.-R. Hou, J. H. Reibenspies, K. Burgess, *J. Am. Chem. Soc.* **2003**, *125*, 113; o) H. Seo, H.-J. Park, B. Y. Kim, J. H. Lee, S. U. Son, Y. K. Chung, *Organometallics* **2003**, *22*, 618; p) L. G. Bonnet, R. E. Douthwaite, B. M. Kariuki, *Organometallics* **2003**, *22*, 4187.
- [5] a) V. César, S. Bellemin-Laponnaz, L. H. Gade, *Organometallics* **2002**, *21*, 5204; b) V. César, S. Bellemin-Laponnaz, L. H. Gade, *Eur. J. Inorg. Chem.* **2004**, 3436.
- [6] a) G. Helmchem, A. Pfaltz, *Acc. Chem. Res.* **2000**, *33*, 326; b) For a general review, covering phosphine-oxazoline ligands in catalysis, see: P. Braunstein, F. Naud, *Angew. Chem.* **2001**, *113*, 702; *Angew. Chem. Int. Ed.* **2001**, *40*, 681.
- [7] Reviews on N-heterocyclic-carbene-transition-metal complexes in asymmetric catalysis: a) M. C. Perry, K. Burgess, *Tetrahedron: Asymmetry* **2003**, *14*, 951; b) V. César, S. Bellemin-Laponnaz, L. H. Gade, *Chem. Soc. Rev.* **2004**, *33*, 619.
- [8] a) D. Enders, H. Gielen, K. Beuer, *Tetrahedron: Asymmetry* **1997**, *8*, 3571; b) W.-L. Duan, M. Shi, G.-B. Rong, *Chem. Commun.* **2003**, 2976; the state of the art in the asymmetric hydrosilylation of ketones with chiral phosphine ligands: c) M. Sawamura, R. Kuwano, Y. Ito, *Angew. Chem.* **1994**, *106*, 92; *Angew. Chem. Int. Ed. Engl.* **1994**, *33*, 111; d) B. Tao, G. C. Fu, *Angew. Chem.* **2002**, *114*, 4048; *Angew. Chem. Int. Ed.* **2002**, *41*, 3892; e) D. A. Evans, F. E. Michael, J. S. Tedrow, K. R. Campos, *J. Am. Chem. Soc.* **2003**, *125*, 3534.
- [9] A preliminary account of this work: V. César, S. Bellemin-Laponnaz, L. H. Gade, *Angew. Chem.* **2004**, *116*, 1036; *Angew. Chem. Int. Ed.* **2004**, *43*, 1014.
- [10] A. I. Meyers, K. A. Novachek, *Tetrahedron Lett.* **1996**, *37*, 1747.
- [11] We also recently reported a very efficient way to synthesise trisoxazolines by using 2-bromooxazoline, see: a) S. Bellemin-Laponnaz, L. H. Gade, *Chem. Commun.* **2002**, 1286; b) S. Bellemin-Laponnaz, L. H. Gade, *Angew. Chem.* **2002**, *114*, 3623; *Angew. Chem. Int. Ed.* **2002**, *41*, 3473.
- [12] A. J. Arduengo, III, F. P. Gentry, Jr., P. K. Taverkere, H. E. Howard, III, US Patent 6 177 575, **2001**.
- [13] See for the different methods: a) C. van der Stelt, DE Patent No. 2130673, **1974**; b) F. G. Bordwell, J. P. Cheng, S. E. Seyedrezai, C. A. Wilson, *J. Am. Chem. Soc.* **1988**, *110*, 8179; c) W. Draber, E. Regel, DE Patent No. 2009020, **1971**.
- [14] A. L. Johnson (E. I. Dupont), U. S. Patent No. 3637731, **1972**.
- [15] C. Köcher, W. A. Herrmann, *J. Organomet. Chem.* **1997**, *532*, 261.
- [16] The formation of the square-planar cationic rhodium species as an active catalyst appears to be crucial, since the use of catalyst **4d** without a silver salt gave poor enantioselectivity and yield (13% ee; 53% yield).
- [17] a) G. Balavoine, J. C. Clinet, I. Lellouche, *Tetrahedron Lett.* **1989**, *30*, 5141; b) Y. Yamanoi, T. Imamoto, *J. Org. Chem.* **1999**, *64*, 2988; c) H. Tsuruta, T. Imamoto, *Tetrahedron: Asymmetry* **1999**, *10*, 877.
- [18] S. Glasstone, K. J. Laidler, H. Eyring, *The Theory of Rate Processes*, McGraw-Hill, New York, **1941**, Chapté 4.
- [19] T. Göbel, K. B. Sharpless, *Angew. Chem.* **1993**, *105*, 1417; *Angew. Chem. Int. Ed. Engl.* **1993**, *32*, 1329.
- [20] J. Brunner, N. Hoffmann, H. D. Scharf, *Tetrahedron* **1994**, *50*, 6819.
- [21] a) H. Buschmann, H.-D. Scharf, N. Hoffmann, M. W. Plath, J. Runsink, *J. Am. Chem. Soc.* **1989**, *111*, 5367; review: b) H. Buschmann, H.-D. Scharf, N. Hoffmann, P. Esser, *Angew. Chem.* **1991**, *103*, 480; *Angew. Chem. Int. Ed. Engl.* **1991**, *30*, 477.
- [22] a) D. Haag, J. Runsink, H.-D. Scharf, *Organometallics* **1998**, *17*, 398; see also: b) D. Enders, H. Gielen, K. Beuer, *Tetrahedron: Asymmetry* **1997**, *8*, 3571.
- [23] a) K. J. Hale, J. H. Ridd, *J. Chem. Soc. Chem. Commun.* **1995**, 357; b) K. J. Hale, J. H. Ridd, *J. Chem. Soc. Perkin Trans. 1* **1995**, 1601.
- [24] I. Ojima, T. Kogure, M. Kumagai, S. Horiuchi, Y. Sato, *J. Organomet. Chem.* **1976**, *122*, 83.
- [25] For a recent kinetic study of hydrosilylation of acetophenone with a rhodium/phosphine catalyst, see: C. Reyes, A. Prock, W. P. Giering, *Organometallics* **2002**, *21*, 546, and references therein.
- [26] The lower yields in the reduction of some of the diakyl ketones are due to the volatility of the products. The conversions are usually complete as determined by ¹H NMR spectroscopy.
- [27] However, we found almost no conversion with this substrate at -60°C. For that reason, the reaction was conducted at -40°C. Complete conversion was observed after 10 h by ¹H NMR spectroscopy.
- [28] a) Q. Jiang, Y. Jiang, D. Xiao, P. Cao, X. Zhang, *Angew. Chem.* **1998**, *110*, 1203; *Angew. Chem. Int. Ed.* **1998**, *37*, 1100; b) R. Kowano, M. Sawamura, J. Shirai, M. Takahashi, Y. Ito, *Bull. Chem. Soc. Jpn.* **2000**, *73*, 485.
- [29] E. W. Abel, M. A. Bennett, G. Wilkinson, *J. Chem. Soc.* **1959**, 3178.
- [30] T. Masuda, J. K. Stille, *J. Am. Chem. Soc.* **1978**, *100*, 268.
- [31] OpenMoleN, Interactive Intelligent Structure Solution, Nonius B. V., Delft (The Netherlands), **1997**.
- [32] G. M. Sheldrick, *Acta Crystallogr. Sect. A* **1990**, *46*, 467.
- [33] G. M. Sheldrick, SHELXL-97, Universität Göttingen (Germany), **1997**.
- [34] A. L. Spek, PLATON, Utrecht University (The Netherlands), **1980-2004**; A. L. Spek, *Acta Crystallogr. Sect. A* **1990**, *46*, C31.

Received: February 7, 2005
Published online: March 3, 2005